Accepted Manuscript

A Systematic Approach for Modeling of Waterflooding Process in the Presence of Geological Uncertainties in Oil Reservoirs

Farzad Hourfar , Karim Salahshoor , Hosein Zanbouri ,
Ali Elkamel , Peyman Pourafshary , Behzad Moshiri

PII: S0098-1354(17)30442-8
DOI: 10.1016/j.compchemeng.2017.12.012
Reference: CACE 5979

To appear in: *Computers and Chemical Engineering*

Received date: 24 June 2017
Revised date: 16 November 2017
Accepted date: 22 December 2017

Please cite this article as: Farzad Hourfar , Karim Salahshoor , Hosein Zanbouri , Ali Elkamel , Peyman Pourafshary , Behzad Moshiri , A Systematic Approach for Modeling of Waterflooding Process in the Presence of Geological Uncertainties in Oil Reservoirs, *Computers and Chemical Engineering* (2018), doi: 10.1016/j.compchemeng.2017.12.012

Highlights

- A system theory-based modeling approach for waterflooding process in oil reservoirs is proposed.
- Impact of geological uncertainties on hydrocarbon recovery efficiency is modeled and quantified.
- System identification, Monte-Carlo Simulations and pattern recognition have been used in the algorithm.
- Reservoir management goals can be pursued in the presence of uncertainty, based on the obtained model.
- Developed approach has been evaluated in MRST environment on 10th SPE-model#2.

A Systematic Approach for Modeling of Waterflooding Process in the Presence of Geological Uncertainties in Oil Reservoirs

Farzad Hourfar[a,1*,2], Karim Salahshoor[b], Hosein Zanbouri[b], Ali Elkamel[c,1*], Peyman Pourafshary[d, 3], Behzad Moshiri[a]

[a] Control & Intelligent Processing Center of Excellence (CIPCE), School of Electrical & Computer Engineering, University of Tehran, Tehran, Iran

[b] Department of Automation & Instrumentation Engineering, Petroleum University of Technology, Ahwaz, Iran

[c] Department of Chemical Engineering, University of Waterloo, Ontario, Canada

[d] School of Chemical Engineering, University of Tehran, Tehran, Iran

Abstract:

In this paper, a systematic approach which is able to consider different types of geological uncertainty is presented to model the waterflooding process. The proposed scheme, which is based on control and system theories, enables the experts to apply suitable techniques to optimize the production. By using the developed methodology, a reasonable mapping between defined system inputs and outputs in frequency domain and around a specific operating point is established. In addition, a nominal model for the process as well as a lumped representation for uncertainty effects are provided. Based on the proposed modeling mechanism, reservoir management goals can be pursued in the presence of uncertainty by utilization of complicated control and optimization strategies. The developed algorithm has been simulated on 10th SPE-model#2. Observed results have shown that the introduced methodology is able to effectively model the dynamics of waterflooding process, while taking into account the assumed induced geological uncertainty.

[1] Corresponding Authors: Farzad Hourfar (f.hourfar@ut.ac.ir), Ali Elkamel (aelkaeml@uwaterloo.ca)

[2] Present Address: Visiting Scholar at Department of Chemical Engineering, University of Waterloo, Canada

[3] Present Address: Department of Chemical & Petroleum Engineering, Sultan Qaboos University, Oman

Keywords*:* Waterflooding Process; Uncertainty Quantification; System Identification; Robust Control and Optimization; Geological Realization of Reservoir; *K-means* Clustering

1. Introduction:

It is predicted that the world energy demand will increase by 50% until 2030, and will be near 300 million barrels per day of petroleum equivalent (ExxonMobil, 2004). On the other hand, oil and gas are still the prevailing available sources to satisfy more than 60% of the current energy global demand. That value is estimated to remain approximately constant for the coming years. Hence, the importance of doing research on different aspects of hydrocarbon energy is undeniable. Although hydrocarbon resources seem to be adequate to meet the increasing request in future decades, it will become more difficult to satisfy the growing demand for oil and gas due to their non-renewable nature. In addition, most of the available reservoirs are almost mature and exploration for large new fields is becoming more and more complicated. These facts attract much attention to enhanced/improved oil recovery (*EOR/IOR*) concepts to increase the production efficiency (Sarma, 2006; Tavallali et al., 2013; Giuliani and Camponogara, 2015; Tavallali and Karimi, 2016a; Zhang et al, 2017).

Oil and gas companies always intend to manage the reservoir to increase the fiscal benefits, even under the presence of inherent geological uncertainties. To this aim, quantifying the effects of uncertainties is really important for the decision makers. Recent achievements in computing and measuring technologies along with the novel progresses in practical methodologies enable the reservoir experts to make more accurate and reliable decisions. Hence, reservoir modeling approaches, which are capable of considering the inherent uncertainties and also being used in reservoir management strategies, have become active research areas in recent years (Gaasø et al., 2014; Tavallali and Karimi, 2016b).

To reduce the influence of uncertainty over the reservoir behavior, surveillance operations are regularly performed for accurate data collection. The gathered data can be used in reservoir management optimization by being incorporated to the commercial simulators to construct the model for estimating the reservoir future behavior. Unfortunately, existing uncertainty in the available information adversely affects the reliability of the obtained results from the simulator. So, establishment of an appropriate mapping between the quantified uncertainty and the gathered production data can be a serious concern (Le and Reynolds, 2014).

In general, "history matching" is a well-known solution for tackling with the challenging task of reliable subsurface characterization. In history matching *(HM)*, the parameters of the model are adjusted such that the model regenerates the recorded data with acceptable accuracy. It should be noted that direct simulation of flow and transport phenomena in heterogeneous media is computationally expensive. So, representation of subsurface uncertain characteristics, for being used to evaluate the reliability of model"s outputs, is of paramount importance in history matching procedure. Accurate statistical description of the reservoir, which should be consistent with available measured data, requires the engagement in valid parametrization of subsurface uncertain characteristics (Ginting et al., 2014). Nowadays, spatial statistical techniques have attracted a wide attention to characterize the uncertainty in hydrocarbon reservoirs. Generally, random field generators are used to represent the range of possible spatial subsurface patterns (Feyen and Caers, 2006). In addition, inverse modeling techniques based on dynamic data are among the common solutions to represent the dynamics of the reservoir (Oliver and Chen, 2011; Zhou et al., 2014). In inverse modeling, calculating the complex nonlinear relationship between model parameters and the data often requires the solution of CPU demanding partial differential equations (PDE"s). This fact may limit the utilization of those techniques in practice. In addition,

due to the ill-posedness nature of the inverse modeling problem, which is basically caused by nonlinearity and lack of enough recorded dynamic data, availability of a spatial prior model is mandatory. Neglecting prior knowledge such as petrophysical properties can result in the models that are geologically unrealistic and have limited predicting capability. So, developing models or inverse solutions that span a realistic range of uncertainty is among the main concerns for the modelers (Caers, 2012). In recent contributions, it has been demonstrated that time-consuming inverse reservoir modeling may not always be necessary for prediction of reservoir behavior (Satija, A., Caers, 2014; Scheidt et al., 2015). This fact stimulates further research to look for fast modeling techniques with the ability of uncertainty handling and also be applicable in reservoir studies such as future production estimation. With few drilled wells, reservoir heterogeneity and also limited available information, acceptable modeling of uncertainty effects is a critical prerequisite to plan for drilling new wells or to define optimal production profiles (Park et al., 2013). The initial step to analyze uncertainty influences on hydrocarbon recovery efficiency is to precisely specify the relationship between uncertain parameters and the recovery factor (Larue and Hovadik, 2008). Generally, thorough and comprehensive earth models are usually used in waterflooding simulation by commercial simulators to accurately estimate the value of recovery factor, amounts of produced oil and water during the operational life, and to make efficient decisions for production optimization purposes. In other words, reservoir comprehensive models provide the essential framework for any type of flow analysis in the reservoir (Hovadik and Larue, 2011). For example, grid-based simulation (Aziz and Settari, 1979; Fanchi, 2001) and streamline simulation (Sayyafzadeh et al., 2010; Shook and Mitchell, 2009) are considered as the most accurate techniques in reservoir modeling and simulation studies. These modeling approaches are mostly used to predict the future behavior of the reservoirs in professional

simulators. The mentioned methods require large amounts of available data and high computational power.

Fortunately, forecasting the dynamic behavior of the reservoir and estimating the recovery factor are also possible by using other faster alternatives such as considering the existing analogy with similar reservoirs possessing similar characteristics (Larue and Yue, 2003), applying decline curve method (Li and Horne, 2005), or utilizing qualitative techniques (Hovadik and Larue, 2011; Shook and Mitchell, 2009; Tang and Liu, 2008). In addition, development of proxy/surrogate models with acceptable accuracy based on available production data is another popular solution due to less computational load (Tafti et al., 2013; Mohaghegh and Abdulla, 2014; Aifa, 2014; van Essen et al., 2012; Sayyafzadeh et al., 2011; Ahmadloo et al., 2010; Elkamel, 1998; Nashawi and Elkamel, 1999).

In the presence of inherent uncertainty in the reservoir, the outcomes from the mentioned modeling approaches may not be as reliable as expected. Hence, any made decision based on non-reliable outputs will not lead to optimal results. For example, design of any controller or optimizer in that situation might be totally ineffective. In other words, simulation the waterflooding process, while ignoring the reservoir uncertainties in the considered model may lead to sub-optimal or even impractical results in practice.

In this paper, through employment of production data a novel algorithm for taking into account the geological uncertainties in modeling of waterflooding process in oil reservoirs has been developed. From system theory point of view, the introduced unstructured uncertainty modeling technique can centralize the uncertainty effects on each desired variable by introducing a specific perturbation module. Consequently, instead of prevalent method of generating multiple realizations to represent a hydrocarbon reservoir containing different uncertainty sources (Siraj et

al 2016; van Essen et al., 2009; Yasari et al., 2013), the proposed modeling procedure, can be utilized. A Monte-Carlo based experiment has been applied in data gathering phase to generate and record the required data-set. Based on the distribution and the number of the uncertain parameters, the data collection experiments have been designed. The set of the plausible linear models, Ω_a, and the nominal reservoir model, G_n, have been obtained in the form of transfer function/matrices by using available data, *K-means* clustering algorithm, and also considering the reservoir as a Multi-Input/Multi-Output (MIMO) system. The mentioned models represent the mapping between system inputs and outputs in the frequency domain around a specific operating point. In addition, the best perturbation module, Δ, has been estimated such that the cumulative $G_n - \Delta$ structure represents the reservoir dynamic behavior in the presence of uncertainty. The proposed modeling approach, which is an extension on (Hourfar et al., 2016), has been evaluated for a set of different reservoir realizations based on 10^{th} SPE-model#2 benchmark as a well-known case study, while assuming that the exact knowledge on the values of permeability parameters is uncertain. The obtained results demonstrate that the developed technique can effectively represent the dynamics of waterflooding process in the presence of geological uncertainties. This characteristic will be useful to construct the models which are applicable in advanced reservoir management strategies, while using robust control and optimization theories.

2. Reservoir Modeling:

Availability of a reliable model is necessary to perform an effective reservoir management. So, constructing appropriate models suitable for different applications is a critical task. In this part, two different approaches for reservoir modeling are briefly discussed.

2.1. Mechanistic Models:

Generally, a hydrocarbon reservoir is modeled by PDE"s based on mass and momentum conservation laws in the professional simulators (Aziz and Settari, 1979; Jansen et al., 2008).

Mass balance for two considered phases (i.e. oil and water) in the reservoir can be described as:

$$\nabla(\rho_i u_i) + \frac{\partial}{\partial t}(\phi \rho_i S_i) = 0; \quad i \in \{o, w\}, \tag{1}$$

in which t is time, ∇ is the divergence operator, ϕ is the porosity, ρ_i is the density of the phase i, u_i is the superficial velocity, S_i is the saturation, defined as the proportion of the pore space occupied by phase i. Moreover, o and w can be used as the notations for oil and water phases, respectively.

In addition, conservation of momentum can be deduced by Navier-Stokes equations. However, the simplified version is described by semi-empirical Darcy's equation for low velocity flow through porous materials as follows (discarding gravity):

$$u_i = -k \frac{k_{ri}}{\mu_i} \nabla p_i, \qquad i \in \{o, w\}, \tag{2}$$

where p_i is the pressure of phase i, k is the absolute permeability, k_{ri} is the relative permeability and μ_i is the viscosity of phase i. The permeability k is an inverse measure of the resistance a fluid encounters flowing in a porous medium. The relative permeability k_{ri} relates to the additional resistance phase i experiences when other phases are present, due to differences in viscosity. Since the relationship between relative permeabilities, k_{ro} and k_{rw}, and water saturation, S_w, is fully non-linear, the reservoir model is a strongly nonlinear system.

Substituting (2) into (1) results into 2 flow equations with 4 unknowns which are p_o, p_w, S_o and S_w. Consequently, two additional equations are required for completing the system description.

The first one states that the summation of phase saturations must be equal to 1:

$$S_o + S_w = 1. \tag{3}$$

The second necessary equation is the capillary pressure equation as:

$$p_{cow} = p_o - p_w = f_{cow}(S_w). \tag{4}$$

In reservoir simulation, it is common to substitute (3) and (4) into the flow equations. Then, by considering oil pressure, p_o, and water saturation, S_w, as primary state variables, we will have:

$$\nabla(\tilde{\lambda}_o \nabla p_o) = \frac{\partial}{\partial t}(\phi \rho_o \cdot [1 - S_w]), \tag{5}$$

$$\nabla(\tilde{\lambda}_w \nabla p_o - \tilde{\lambda}_w \frac{\partial p_{cow}}{\partial S_w} \nabla S_w) = \frac{\partial}{\partial t}(\phi \rho_w S_w), \tag{6}$$

where $\tilde{\lambda}_o = k\frac{k_{ro}}{\mu_o}$ and $\tilde{\lambda}_w = k\frac{k_{rw}}{\mu_w}$ are called oil and water mobilities. Flow equations (5) and (6) are defined over the entire volume of the reservoir. It is supposed there is no flow across the boundaries of the reservoir geometry over which (5) and (6) are defined (Neumann boundary conditions).

One conventional approach in commercial simulators for solving the above equations is discretization in time and space. That policy results in:

$$\mathbf{V}(\mathbf{x}_k) \cdot \mathbf{x}_{k+1} = \mathbf{T}(\mathbf{x}_k) \cdot \mathbf{x}_k + \mathbf{q}_k, \qquad \mathbf{x}_0 = \bar{\mathbf{x}}_0, \tag{7}$$

where *k* is the time index, $\mathbf{x}$ is the state vector consisting of p_o and S_w in all grids. In addition, $\bar{\mathbf{x}}_0$ is a known vector which contains initial condition values. The effect of the wells on the dynamics of the reservoir can be modeled in (7) by a source vector named $\mathbf{q}_k$.

$$q_k^j = w^j \cdot (p_{bh,k}^j - p_k^j) \ , \tag{8}$$

in which $p_{bh,k}^j$ is the well's bottom hole pressure, *j* is the index of the grid block containing the well and p_k^j is the grid block pressure in which the well is located. In addition, *w* is a constant that quantifies the well's geometric factors and also the rock and fluid properties in the vicinity of the well.

2.2. Black-Box Reservoir Modeling:

Instead of solving the equations presented in section 2.1 for all grids in each time step, system theory-based modeling techniques can be utilized to model the waterflooding process in the framework of fast simulation approaches. This strategy helps to evade from complicated calculations which originate from PDE‟s handling. So, analyzing the reservoir behavior under certain conditions can be performed faster and with lower computational expenses. To this aim, an appropriate linear mapping between production and injection data in the form of transfer function/matrix, either in continuous or discrete space can be found, while assuming the reservoir as a MIMO system (Hourfar et al., 2016, 2017). In this approach, the inputs of the reservoir are well controls, which are generally total injection flow rates or bottom hole pressures (*bhp*) of the wells. Moreover, oil and water production rates of the producing wells are supposed to be the reservoir outputs (Figure1).

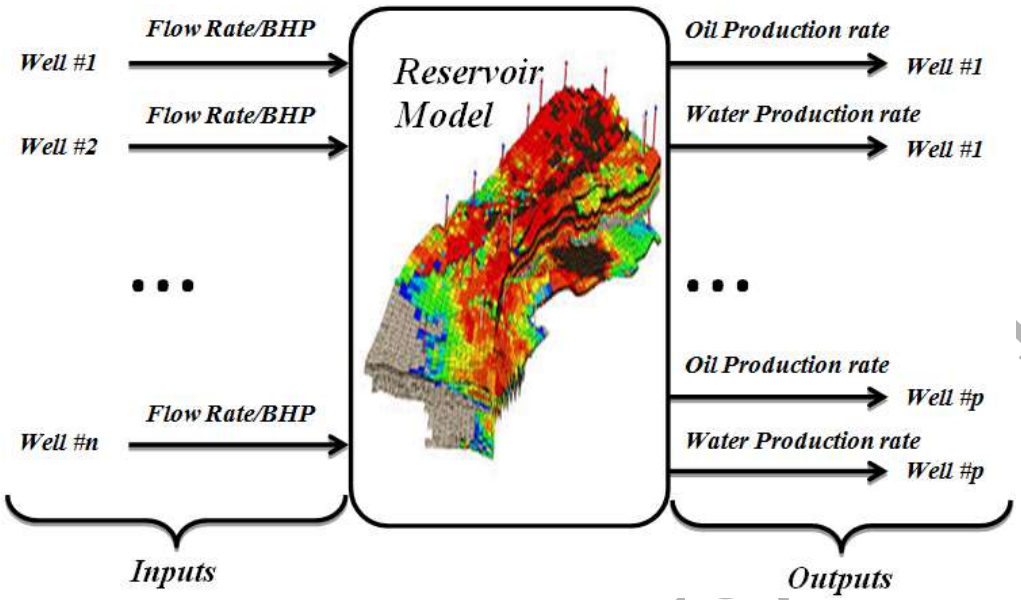

Figure 1. Schematic of oil reservoir as a Multi-Input-Multi-Output system (Hourfar et al., 2016).

Using the unit delay operator, q^{-1} , the oil reservoir can be linearly modelled in each operating point as follows:

$$A(q)y(k) = B(q)u(k), \tag{9}$$

in which y is the *p*-dimensional output vector (oil, water, or total production rate of the producing wells), u is the *m*-dimensional input vector (injection rate or *bhp* of the wells), and $A(q)$ and $B(q)$ are polynomial matrices as:

$$A(q) = I + A_1 q^{-1} + \cdots + A_n q^{-n} \quad . \tag{10}$$

$$B(q) = B_1 q^{-1} + \cdots + B_n q^{-n} \quad . \tag{11}$$

Generally, in MIMO systems (9) can be expresses as:

$$y = G(q)u, \tag{12}$$

in which $G(q) = A^{-1}(q)B(q)$.

Equivalently, by applying Laplace transform, which is normally used for continues and frequency domain representation, the transfer matrix of the reservoir, $G(s)$, can be obtained as:

$$Y(s) = G(s)U(s). \tag{13}$$

It should be clarified that the main reason of utilizing Laplace transform in this paper and switching from discrete time domain to frequency domain is to construct a standard structure for waterflooding process, applicable in various types of robust control framework. It has been demonstrated in (Hourfar et al., 2016) that the presented proxy modeling methodology is capable to estimate the desired outputs with acceptable accuracy. However, as it is clear in (1) and (2), the values of internal parameters and characteristics of the reservoir such as porosity or permeability of each grid block generally contain different levels of inherent uncertainty. Hence, the outputs of proxy modeling approaches which ignore the effect of existing uncertainties may not be reliable for real applications.

As a result, in this paper a fast reservoir modeling approach, suitable for waterflooding simulation has been developed such that the parametric uncertainties can be taken into account during the modeling process. In other words, the considered problem in this paper can be expressed as follows:

"Introducing a valid model for waterflooding process with the following characteristics:

a) Being able to reflect the effects of existing geological uncertainties on the production regime during the waterflooding process.
b) Needless to directly challenge with complex PDE"s of the reservoir to estimate the productivity condition, while proposing a data driven proxy modeling technique which is constructed based on available production data.

c) Providing a lumped structure model to represent the probable behaviors of the reservoir in the presence of uncertainty (instead of using a set which includes different reservoir realizations).

d) Capability of being used by advanced control and optimization techniques."

3. Uncertainty Quantification

Typically, uncertainty originates from perturbations which represent the differences between the constructed model and the real system. The discrepancy generally appears due to un-modeled dynamics, ignored nonlinearities in the modeling process, model order reduction, and lack of exact knowledge about parametric values. The above shortcomings have negative effects on controller/optimizer stability and performance during the operation (Gu et al., 2013).

In this paper, a systematic methodology is proposed to quantify the impacts of uncertainty on waterflooding process. The introduced technique provides the facilities to easily model the dynamic behavior of waterflooding process, while internal parameters such as permeability or porosity have different degrees of uncertainty.

3.1. Unstructured Uncertainty Modeling

The main goal in this paper is to consider all dynamic perturbations as a single perturbation block, Δ, in the constructed model. This kind of uncertainty representation is known as "unstructured" uncertainty modeling in the literature. In linear, time-invariant (LTI) systems, the block Δ would be an unknown transfer function matrix. Although the unstructured uncertainty can be presented in various forms, additive uncertainty modeling structure is introduced in this section. In additive uncertainty modeling scheme of single input single output (SISO) systems, the relationship between the transfer function of the real perturbed system dynamic, $G_P(s)$,

and the nominal model of the physical system, $G_o(s)$, is as (14) in the presence of uncertainty, $\Delta(s)$:

$$G_P(s) = G_o(s) + \Delta(s). \tag{14}$$

If the system is MIMO, the mentioned transfer functions will change to a transfer matrix. Figure 2 demonstrates the general schematic of additive uncertainty modeling structure.

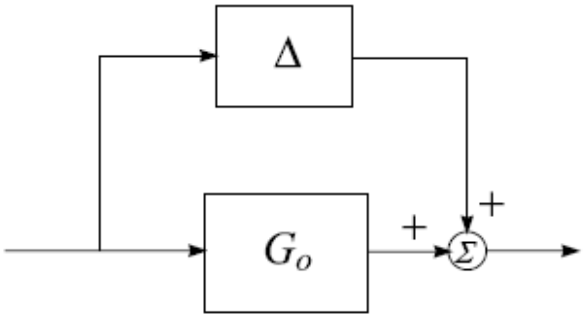

Figure 2. Additive uncertainty configuration of an uncertain system.

Generally, in additive uncertainty representation, quantifying the value of absolute error between the actual dynamics and the outputs of nominal model is a crucial step. Although the term $\Delta(s)$ in (14) is uncertain and its exact value is unknown, it can be bounded by a known transfer function, which means $\bar{\sigma}[\Delta(j\omega)] \le \delta(j\omega)$, for all frequencies ω, where δ is a known scalar function and $\bar{\sigma}[\Delta(j\omega)]$ is the notation for the largest singular value of the uncertainty matrix. Consequently, the uncertainty of the considered system can be lumped in a unit, norm-bounded block, Δ, which is followed by a scalar transfer function $\delta(s)$. For more clarification, by taking into account the nominal transfer function of the system as $G_o(s)$, the actual transfer function given by $G(s)$, and assuming the difference between nominal and real model, $G(s) - G_o(s)$, is stable, the model uncertainty can be represented by using a bound of the following form:

$$\left|G(j\omega)-G_o(j\omega)\right|\le \ell_a(\omega), \tag{15}$$

in which ℓ_a stands for uncertainty radius at each frequency, ω.

(15) expresses that the response of actual system, $G(s)$, lies in a band of uncertainty which is located in the vicinity of the obtained results from the nominal transfer function, $G_o(s)$. Since no phase information in error modeling is incorporated, the explained approach for uncertainty modeling mostly leads to conservative results.

Based on the above description, the following uncertainty set is defined for additive uncertainty modeling:

$$\Omega_a=\left\{G(s)\middle|\, G(s)=G_o(s)+W_a(s)\Delta_a(s)\right\}, \tag{16}$$

where Δ_a is an arbitrary stable transfer function which should satisfy the following norm condition:

$$\left\|\Delta_a\right\|_\infty=\sup_\omega\left|\Delta_a(j\omega)\right|\le 1 \ . \tag{17}$$

Considering inequality (18), the stable proper rational weighting term, $W_a(s)$, is utilized to demonstrate any available information about the accuracy of the nominal model.

$$\left|W_a(j\omega)\right|\ge\left|W_a(j\omega)\Delta_a(j\omega)\right|=\left|G(j\omega)-G_o(j\omega)\right| \ , \tag{18}$$

or equivalently,

$$\left|W_a(j\omega)\right|\ge\max_{G\in\Omega_a}\left|G(j\omega)-G_o(j\omega)\right|=\ell_a(j\omega) \ . \tag{19}$$

Figure 3 illustrates the internal configuration of G as the actual system based on its principal components which are: G_o, W_a, and Δ_a.

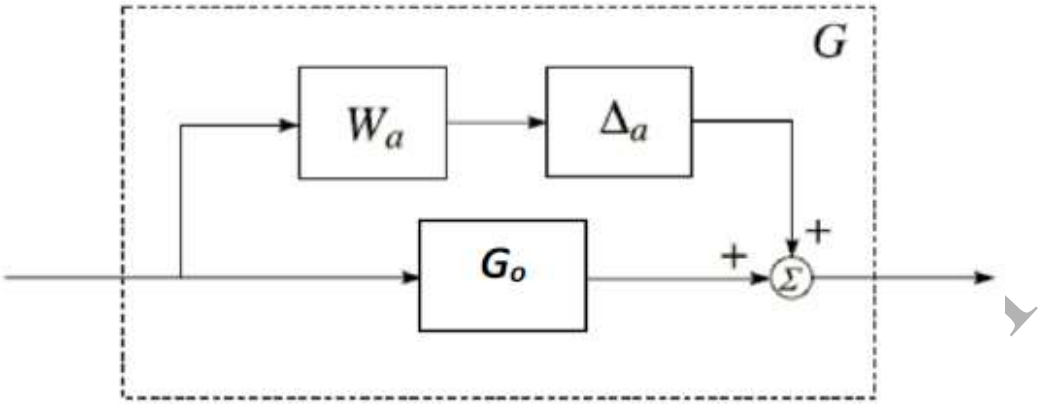

Figure 3. Configuration of G_o, W_a, and Δ_a in additive uncertainty modeling structure.

It should be noted, it is necessary that the unstable poles of available models in Ω_a are matched with those of the nominal model. Consequently, the utilized identification techniques should be able to successfully detect the unstable poles of the system. By taking into account the knowledge about the lower bound, $\ell_a(j\omega)$, it is possible to explore for a stable weighting function, $W(s)$, such that:

$$\left|W_a(j\omega)\right| \geq \ell_a(j\omega) \quad . \tag{20}$$

In practical applications, accurate perturbation modeling is an important prerequisite to design an appropriate controller/optimizer in the presence of uncertainties (Grossmann et al., 2016). In other words, the introduced modeling structure can be considered as a basic form in well-known robust control approaches. By using the proposed model, challenging problem of wateflooding optimization can be formulated for instance as an H_∞ controller design. That policy is a good alternative to evade from time-consuming common robust optimization techniques, in which the optimization problem should be solved for all available reservoir realizations. Figure 4 demonstrates the closed-loop structure for utilizing the developed model in regular robust control

framework. In Figure 4, *K* stands for the controller/optimizer. In addition, *w* and *z* are considered as process inputs and outputs, while, *y* and *u* are controller inputs and outputs, respectively.

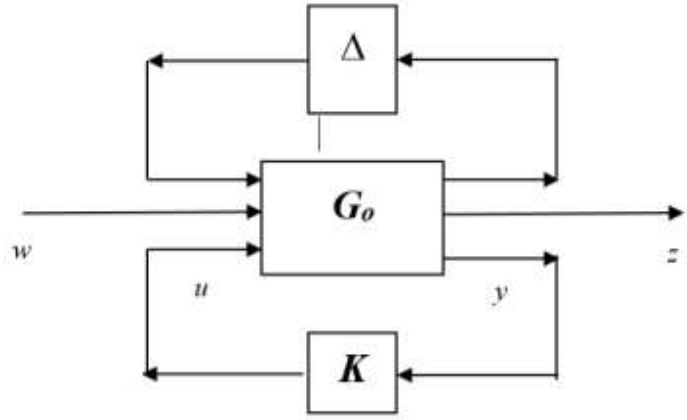

Figure 4. General structure of utilizing developed model in robust controller/optimizer design.

4. Methodology of Waterflooding Process Modeling in the Presence of Uncertainty

In this section, the proposed methodology which has been compatible to model the waterflooding process in the presence of uncertainty in oil reservoirs is explained in detail. The introduced approach is subdivided into three separate steps as:

4.1. Initialization

At the initial step, system inputs and outputs for modeling purposes are specified. The algorithm tries to find a proper mapping between inputs and outputs, based on the available data while taking into account the inherent reservoir uncertainties. To this aim, the reservoir parameters are divided into two sets: 1) certain and, 2) uncertain. The former parameters are the ones that exact knowledge about their values is available and the latter are those which contain some sort of uncertainty.

4.2. Data Generation and Uncertainty Realization in the Reservoir Simulator

In all data-driven modeling approaches proper input-output data collection is one of the most important sections for representing the dynamics of the system with high accuracy. The richer

the gathered data, the better the obtained model. So, in this phase it is mandatory to stimulate the reservoir such that most of the hidden dynamics are identified. Theoretically, Persistently Exciting (PE) signals are suitable candidates to be applied as system inputs. In general, white noise and Pseudo Random Binary Signal (PRBS) can be considered as inputs with PE characteristics. However, applying fully PE inputs is not a practical solution due to it is not recommended to regularly re-adjust the setting of control valves with high frequencies during oil production. So, an alternative which meets the operational constraints and also mimics PRBS characteristics should be utilized as the system input. Afterwards, data pre-processing should be done over the set of collected input/output data for numerical robustness enhancement as well as accelerating the convergence speed of modeling.

To calculate the effect of uncertain parameter on the reservoir behavior- such as production regime- that parameter should be applied in the valid simulator. So at the first stage, the characteristics of uncertain parameter should be determined. An applicable expression for an uncertain-parameter, θ , is as follows:

$$\theta = \frac{\theta_o(100 \pm \alpha)}{100}, \tag{21}$$

in which θ_o is the nominal value of the uncertain parameter and α is the percentage of deviation from θ_o. Without loss of generality, in this paper it has been assumed that the uncertain parameter has uniform distribution or equivalently its corresponding probability density function (*pdf*) is:

$$p(\theta) = \begin{cases} \dfrac{1}{b-a} & \text{for } a \le \theta \le b \\ 0 & \text{otherwise} \end{cases}, \tag{22}$$

where $b = \theta_o + \frac{\theta_o \times \alpha}{100}$ and $a = \theta_o - \frac{\theta_o \times \alpha}{100}$.

By considering the dimension and the distribution of the assumed uncertainty, minimum required number of simulations, *N*, which can reflect the probable dynamic behavior of waterflooding process in the presence of existing uncertainty, will be specified. Needless to mention, this approach originates from Monte Carlo experiment methodology. *N* should be selected such that the set of obtained outputs from different experiments, appropriately represents the effect of considered uncertainty in the output space. It should be noted that Like other Monte-Carlo based techniques, increasing the number of experiments, *N*, leads to a better estimation of uncertain or stochastic process. So, it can be concluded that a larger *N* is equivalent with more reliable model. However, some factors such as available computational power, required accuracy relevant to a specific application, tolerable errors between the output of generated model and the real output, size of the considered reservoir and also the pattern of uncertain parameter distribution may result in different acceptable values in selecting "*N*". In other words, by taking into account the mentioned factors, the field expert is free to choose the value of *N* such that the trend of obtained results acts as an acceptable representative for the dynamic of the system in the presence of considered uncertainty. So at this phase, a set of uncertain parameters with *N* members are randomly generated while all members satisfy (21) or (22). By applying proper input signal which can be water injection sequence, the generated θ"s are used in *N* different simulations. Meanwhile, the production data which are the system outputs (oil production, water production or total production of the wells) will be recorded to build the set of relevant input/output data in the presence of parameter θ uncertainty.

4.3. Model Development

In this stage, each set of input/output data, generated by the reservoir simulator at a specified value of uncertain parameter θ, is used to find an appropriate linear input/output mapping in the form of transfer function. This implies that the set of transfer function models represent the dynamic of the waterflooding process when the value of θ varies according to (21). For more details about computation of data-driven transfer function modeling in oil reservoirs, based on available injection/production data and also advantages and limitations of that technique, one may refer to (Sayyafzadeh et al., 2011; Hourfar et al., 2016).

4.3.1. Nominal Transfer Function Computation

After calculating the transfer functions "$G_i(s):\ i=1,\ldots,k$" related to all simulations and constructing the following set, Γ:

$$\Gamma=\{G_1(s),G_2(s),\ldots,G_k(s)\}, \tag{23}$$

in which *k* is the number of experiments corresponding with different θ"s, the nominal transfer function for waterflooding process, $G_o(s)$, can be easily obtained in the next step.

Generally, the identified transfer function for the i^{th} experiment, $G_i(s)$, is represented as follows:

$$G_i(s)=\frac{N(s)}{D(s)}=\frac{b_{m,i}s^m+b_{m-1,i}s^{m-1}+\cdots b_{0,i}}{s^n+a_{n-1,i}s^{n-1}+\cdots+a_{0,i}}\ . \tag{24}$$

It is possible to factor the numerator, $N(s)$, and the denominator, $D(s)$, polynomials for expressing the transfer function as follows:

$$G_i(s)=K_i\frac{(s-z_{1,i})(s-z_{2,i})\cdots(s-z_{m-1,i})(s-z_{m,i})}{(s-p_{1,i})(s-p_{2,i})\cdots(s-p_{n-1,i})(s-p_{n,i})}\ . \tag{25}$$

where $N(s)$ and $D(s)$ have real coefficients defined based on system"s differential equation and $K_i=b_{m,i}$. The z_i"s are the roots of $N(s)$ and are called system or transfer function zeros.

The p_i"s are the roots of $D(s)$ and are called system or transfer function poles. Since all the coefficients of $N(s)$ and $D(s)$ are real, the poles and zeros must be either purely real, or appear in the format of complex conjugate pairs.

Although some attempts have been done to quantify the uncertainty in the form of transfer functions in several applications (de Vries and van den Hof, 1995; Douma and van Den Hof, 2005; Ko et al., 2008), in this paper we present an algorithm tailored to be suitable in waterflooding process.

By assuming the number of zeros and poles do not change in all G_i"s (i.e. the orders of nominators and denominators remain constant for all transfer functions) and also supposing that the presence of uncertainty does not cause any variation in the nature of stable/unstable poles or minimum/non-minimum phase zeros, the nominal transfer function, $G_o(s)$, is calculated based on *k-means* clustering algorithm (Kanungo et al., 2002). The above assumptions can be interpreted as:

A1) The uncertainty does not affect the assumed structure of the system during the modeling process.

A2) The uncertainty does not change the critical behavior of the system.

In other words, the presented algorithm can appropriately work when the above conditions are satisfied. For example, if the uncertainty causes any change in the number of poles or zeros, then a fixed structure for the transfer function cannot be assumed as the model of the process. In addition, if the uncertain parameter forces one or more poles(zeros) to cross over the imaginary axes, then *k-means* clustering algorithm is unable to introduce an acceptable representative for those poles(zeros). The reason of the mentioned inability is that there exists no pole(zero) which can be a valid representative for both stable and unstable poles(zeros), simultaneously.

At this point, the nominal transfer function of waterflooding process should be calculated such that it acts as an acceptable representative for all of the observed experiments. The interpretation of the mentioned statement is to locate poles(zeros) of $G_o(s)$ in *s*-plane such that each pole(zero) appropriately represents the corresponding cluster of poles(zeros) of the members of set *Γ*. To this aim, *k-means* clustering technique is applied to properly calculate the locations of poles(zeros) of $G_o(s)$ by performing the following steps:

- Identifying the groups of poles and zeros correctly, which can be done by assuming K_n distinct clusters based on the order of $D(s)$ for poles clustering, and K_m distinct clusters based on the order of $N(s)$ for zeros clustering.
- Finding suitable representatives, which would be the poles and zeros of $G_o(s)$, corresponding to determined clusters. The representatives are normally chosen as the cluster centers, *μ*.

To obtain a proper cluster center, the summation of the cluster members" distances- e.g. in the form of Euclidean distance- from the cluster center is minimized:

$$L = \sum_{j=1}^{K} \sum_{i} \left\| x_i - \mu_j \right\|^2, \tag{26}$$

where x_i is assigned to cluster *j* and *K* is the number of clusters which for pole-clusters is equal to K_n and for zero- cluster is equal to K_m.

Equivalently, *L* can be expressed as follows:

$$L = \sum_{j=1}^{K} \sum_{i=1}^{p} a_{ij} \left\| x_i - \mu_j \right\|^2$$
$$\text{where } a_{ij} = \begin{Bmatrix} 1 \text{ if } x_i \text{ assigned to cluster } j \\ 0 \text{ else} \end{Bmatrix}, \tag{27}$$

and p is the number of all points (poles or zeros).

The ultimate goal is minimizing L, based on properly choosing a_{ij}"s and μ"s. In other words, by minimization of the value of L, the center of each cluster is determined. This task can be done iteratively in different steps:

1- Initializing the values of μ_1 ..... μ_k arbitrarily.

2- Choosing optimal a_{ij},,s for fixed μ"s.

3- Choosing optimal μ"s for fixed a_{ij}.

4- Repeating 2 and 3 until convergence.

Assigning x_i to the nearest μ_j, results in the following a_{ij}"s:

$$a_{ij} = \begin{Bmatrix} 1 \;\; if \;\; j = \arg\min_l \left\| x_i - \mu_l \right\|^2 \\ 0 \;\; else. \end{Bmatrix} , \tag{28}$$

and for calculating the μ"s, the following condition should be satisfied:

$$\nabla_{\mu_j} L = 0 ; \tag{29}$$

which results in:

$$\mu_j = \frac{1}{n_j} \sum_i x_i , \tag{30}$$

where n_j is the number of x_i, assigned to cluster j.

In the s-plane, the interpretation of (30) is to compute mean values for real and imaginary parts of pole and zero clusters.

4.3.2. Weighting Transfer Function Estimation

As explained in section 3, system transfer function in the presence of uncertainty related to the i^{th} experiment, $G_i(s)$, can be expressed as:

$$G_i(s) = G_o(s) + \Delta_i(s), \tag{31}$$

where $G_o(s)$ is the nominal transfer function, and $\Delta_i(s)$ is the uncertainty model in the format of transfer function for the i^{th} experiment and can be expressed as (32) based on (16):

$$\Delta_i(s) = W(s)\Delta'. \tag{32}$$

Consequently, the dynamic of the uncertain part is presented by $W(s)$ and norm of Δ' is considered to be no more than 1, which means $\|\Delta'\| \le 1$.

As a result, the following inequality should be satisfied in all frequencies:

$$\forall G_i, s: \ \|G_i(s)\| = \|G_o(s) + W(s)\Delta'\| \le \|G_o(s)\| + \|W(s)\Delta'\| \le \|G_o(s)\| + \|W(s)\|. \tag{33}$$

It should be noted that the system norm or transfer function norm, $\|G\|$, which is equivalent to maximum system gain, is defined as:

$$\|G\| := \underset{u \neq 0}{Sup} \frac{\|Gu\|_Y}{\|u\|_U}. \tag{34}$$

in which G is a transfer function for a linear and bounded system that maps the input signal, $u(t)$, to the output signal, $y(t)$, and $u \in (U, \|.\|_U)$, $y \in (Y, \|.\|_Y)$. U and Y are the signal spaces with the specified norms $\|.\|_U$ and $\|.\|_Y$, respectively.

To determine $W(s)$ based on the above explanations, it is necessary to plot Bode magnitude diagram of the error frequency responses, $E_i(j\omega)$"s, for all available G_i"s in different frequencies, ω.

$$E_i(j\omega) = G_i(j\omega) - G_o(j\omega). \tag{35}$$

Afterwards, $W(s)$, should be designed and shaped with minimum possible order such that it acts as an envelope over the E_i"s in all frequencies.

The flowchart of this methodology is illustrated in Figure 5.

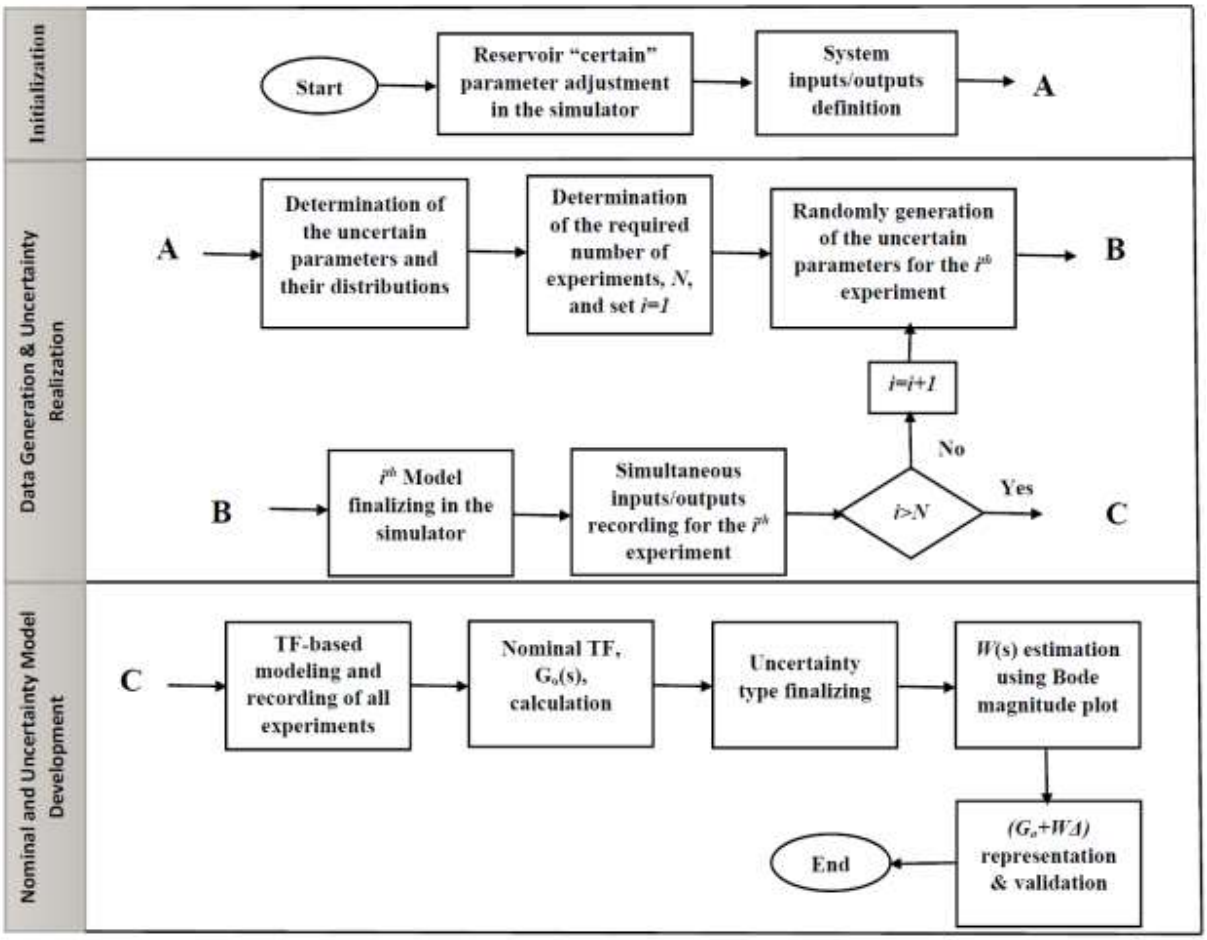

Figure 5. Flowchart of the presented methodology.

5. Algorithm Implementation and Results

The developed algorithm has been implemented in Matlab Reservoir Simulation Toolbox (MRST) environment (Lie, 2014). Using MRST provides the capability of controlling and optimizing the reservoir production by properly adjustment of the manipulated variables which

are normally selected as well flowrate or *bhp*. It should be clarified here that in "well control section" of the simulator, the initial values of *bhp*"s dedicated to the producing wells are all specified. Then, by continuously adjusting the water flow rate of injection wells, the defined outputs are recorded. The outputs of the system which are going to be modeled in the presence of uncertainty are generally supposed to be oil and water production rates of producing wells. Furthermore, in order to prevent from over-pressurization in the reservoir, the following equality constraint is always satisfied:

$$\sum_{i=1}^{m} q_{i\_inj} = \sum_{j=1}^{p} q_{j\_prod} \,, \tag{36}$$

where q_{i_inj} is the flowrate of each injection well, q_{j_prod} is the total flowrate of each producing well, m is the number of injection wells and p is the number of production wells.

After initialization and adjustment of the required parameters, variables such as total production rate, oil production rate, water production rate and water cut of all producing wells are computed at each time-step by the simulator. Due to the existing correlation in the generated outputs, modeling just two variables from the mentioned list is sufficient to estimate the others. Hence, in this section it is enough to demonstrate the modeling results of "total production" and "oil production" of producing wells.

The proposed algorithm is applied to the well-known 10th SPE-Model#2 for waterflooding process modeling, including induced geological uncertainty. So, a Single Input, Multi Output (SIMO) model (one injection well and four production wells) is constructed. The porosity and permeability maps for 10th SPE-Model#2 as well as other parameters such as well locations in Cartesian coordinate and initial adjustments are available in (Christie and M. J. Blunt, 2001; Islam and Sepehrnoori, 2013).

An appropriate injection sequence for the period of 2000 days of operation, which satisfies the practical constraints and also has the most analogy with PE signals, has been applied to the reservoir (Sequence of injection rate is available in electronic supplementary material).

We have assumed that the water injection rate can switch to a new value in the interval of [3000*bbls/day*-6000*bbls/day*] just once in 100 days. In addition, the inputs and outputs of the system are recorded every 10-days due to the slow dynamic of the reservoir. So, the corresponding sampling time, T_s, is 864000*s*.

Furthermore, for modeling and estimation of the uncertainty influences on the production regime, we supposed that our knowledge about the exact value of the permeability-as a sample for the source of geological uncertainty- is not precise. In other words, the permeability of each grid in the simulator may deviate up to 10% from its nominal value according to (21).

The obtained results demonstrate that the developed modeling technique is capable to introduce a lumped model structure, applicable in analyzing the effects of induced geological uncertainty on waterflooding process with good accuracy.

Figure 6, shows the general configuration of the constructed model for mimicking the waterflooding process in the studied example. Clearly, the system input (injected water) can affect the defined outputs (total production rates and oil production rates of four producing wells) thorough the nominal and uncertainty transfer functions. Table 1 and 2 contain the computed values of the transfer functions, related to oil production rates and total production rates, respectively.

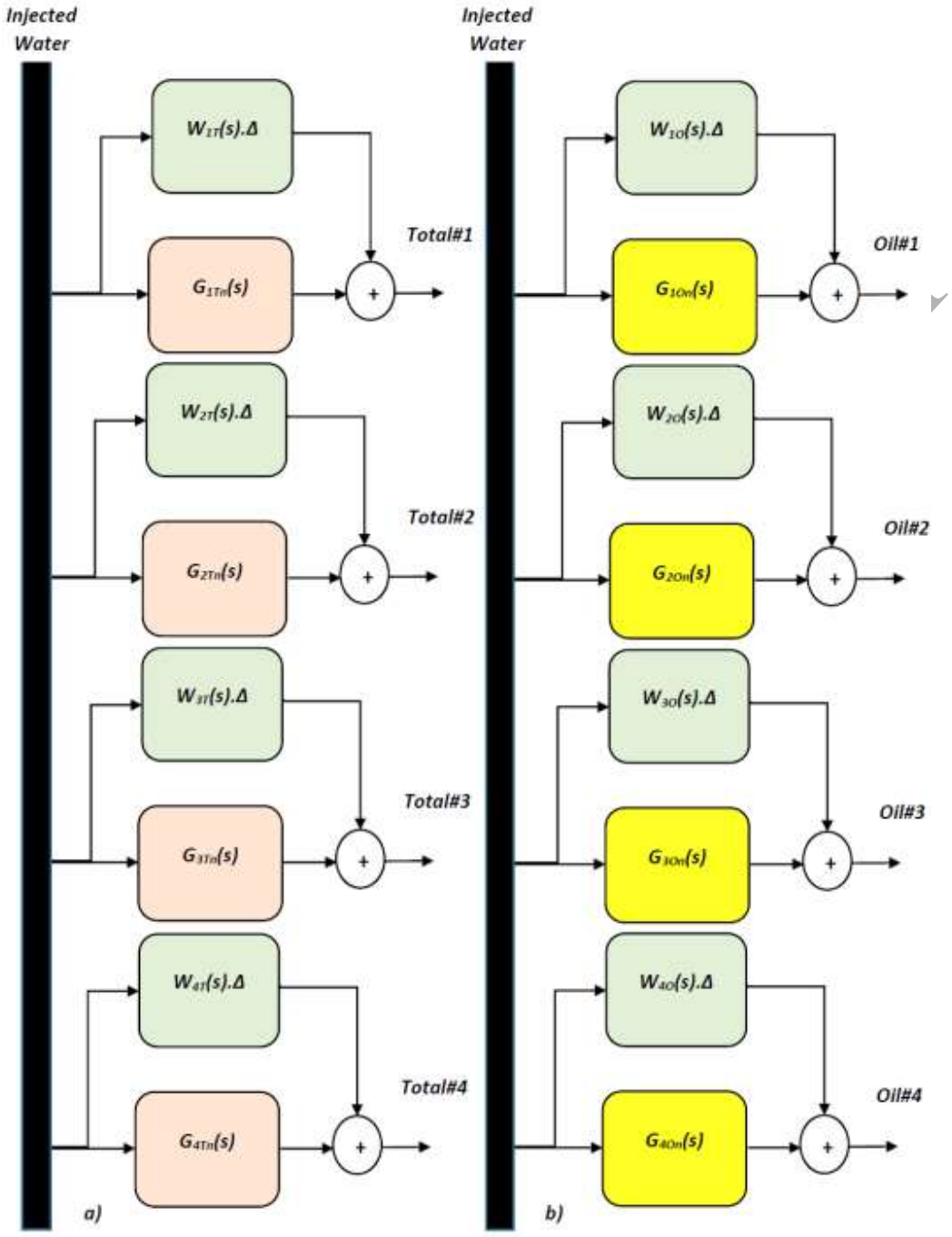

Figure 6. General configuration of systematic uncertainty modeling for waterflooding process from injection well to producing wells (well#1 to well#4) in 10th SPE10-Model#2. a) G_{Tn} *'s* and W_{Tn} *'s* are related to total production rates, b) G_{On} *'s* and W_{On} *'s* are related to oil production rates.

Table 1. Calculated nominal and weighting transfer functions from injection well to all producing wells for "oil production rate" modeling.

Well no.	***Nominal Transfer Functions***	***Weighting Transfer Functions***
#1	$G_n(s)=\frac{(2.52e-8)s^2+(1.128e-14)s^1+(1.026e-22)}{s^3+(5.04e-7)s^2+(2.797e-13)s^1+(4.121e-21)}$	$W(s)=\frac{(6.387e-5)s^3+(1.295e-7)s^2+(3.24e-13)s^1+(1.253e-19)}{s^3+(4.661e-6)s^2+(5.359e-12)s^1+(2.511e-18)}$
#2	$G_n(s)=\frac{(1.94e-7)s^2+(1.374e-14)s^1+(2.296e-22)}{s^3+(2.242e-6)s^2+(2.36e-13)s^1+(5.219e-21)}$	$W(s)=\frac{(6.155e-5)s^3+(1.149e-7)s^2+(1.331e-12)s^1+(1.978e-18)}{s^3+(1.415e-5)s^2+(4.664e-11)s^1+(6.152e-17)}$
#3	$G_n(s)=\frac{(3.16e-7)s^2+(3.173e-14)s^1+(4.45e-22)}{s^3+(2.523e-6)s^2+(3.333e-13)s^1+(7.613e-21)}$	$W(s)=\frac{(0.0003097)s^3+(2.441e-7)s^2+(4.606e-13)s^1+(5.628e-20)}{s^3+(4.02e-6)s^2+(6.241e-12)s^1+(1.049e-18)}$
#4	$G_n(s)=\frac{(8.72e-8)s^2+(1.161e-14)s^1+(1.529e-22)}{s^3+(1.057e-6)s^2+(1.588e-13)s^1+(3.334e-21)}$	$W(s)=\frac{(6.872e-5)s^1+(1.048e-7)}{s^1+(2.411e-6)}$

Table 2. Calculated nominal and weighting transfer functions from injection well to all producing wells for "total production rate" modeling.

Well no.	***Nominal Transfer Functions***	***Weighting Transfer Functions***
#1	$G_n(s)=\frac{(6.001e-8)s^2+(2.236e-14)s^1+(5.013e-22)}{s^3+(6.919e-7)s^2+(2.596e-13)s^1+(5.582e-21)}$	$W(s)=\frac{(0.0001884)s^2+(4.653e-8)s^1+(4.877e-14)}{s^2+(1.061e-6)s^1+(9.439e-13)}$
#2	$G_n(s)=\frac{(2.051e-7)s^2+(1.592e-14)s^1+(6.48e-22)}{s^3+(1.201e-6)s^2+(1.192e-13)s^1+(3.638e-21)}$	$W(s)=\frac{(0.001543)s^1+(2.895e-7)}{s^1+(2.563e-6)}$
#3	$G_n(s)=\frac{(2.83e-7)s^2+(3.615e-14)s^1+(7.074e-22)}{s^3+(6.096e-7)s^2+(1.02e-13)s^1+(1.325e-21)}$	$W(s)=\frac{(0.00268)s^1+(5.906e-7)}{s^1+(2.146e-6)}$
#4	$G_n(s)=\frac{(2.74e-7)s^2+(7.883e-14)s^1+(1.607e-22)}{s^3+(1.239e-6)s^2+(3.908e-13)s^1+(6.187e-22)}$	$W(s)=\frac{(0.0003729)s^1+(3.521e-7)}{s^1+(5.817e-7)}$

For more clear and distinguishable illustration, just the results for 30 random simulations regarding the different uncertain permeability values have been depicted. The following figures demonstrate the outcomes related to each step for one of the considered outputs (oil production of well#3), for the sake of brevity.

Figure 7 shows the water injection profile in the reservoir (system input) which is selected to have pseudo-PE characteristics, while considering the practical constraints on set-point variation frequency.

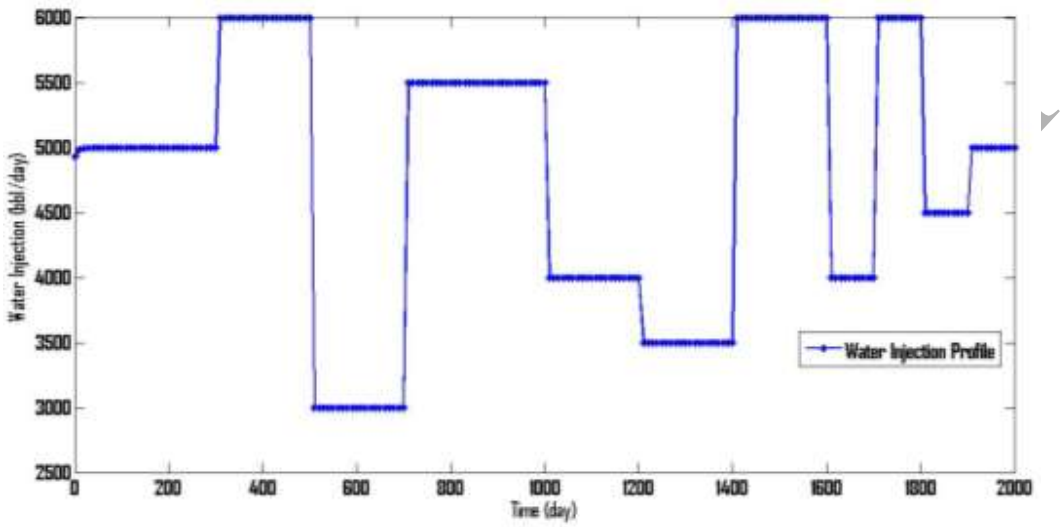

Figure 7. Water injection profile in the reservoir (system input).

Figure 8 illustrates oil production rate of well#3 (as the selected output) in 30 different permeability scenarios, corresponding with simulating the real conditions and the estimated TF models‟ outputs related to each experiment. The TF models are computed in frequency domain such that they provide the best linear approximations around the operating point for all studied scenarios. Despite the nonlinear nature of the reservoir dynamic, the obtained results show that the calculated TF‟s are successful in modeling the output deviations- which are due to the existence of the uncertain parameter- with acceptable accuracy, around the operating point.

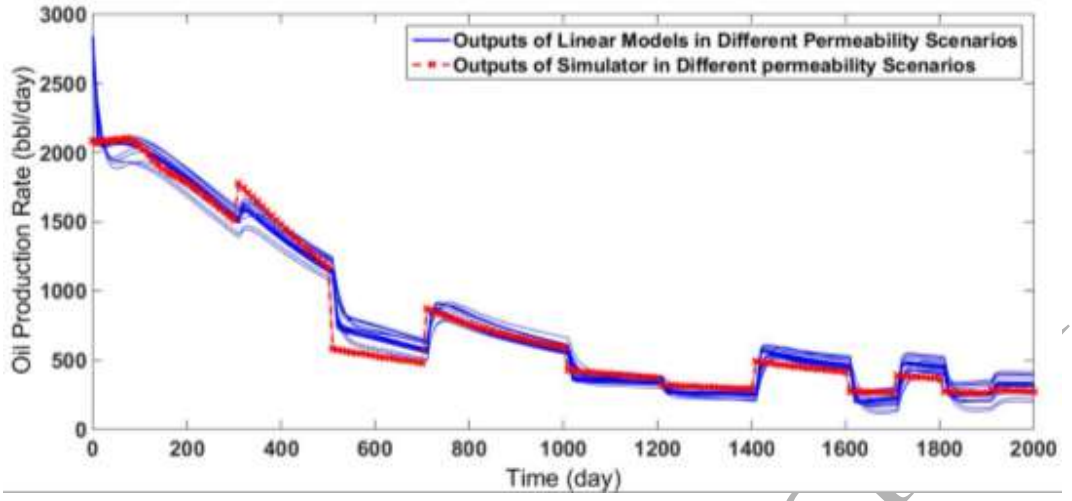

Figure 8. Comparison of simulator outputs and TF models outputs (Considering oil production of well #3 as the modeled output).

By applying the explained technique in section 4.3.1 and also using *k-means* clustering algorithm, the nominal model of the process has been created, while taking into account the calculated transfer functions relevant to all studied scenarios (Table 1). Figures 9 and 10 demonstrate Bode magnitude plots and the time responses of the nominal transfer function as well as the estimated transfer functions, regarding the different permeability scenarios, respectively. It can be observed that the nominal model has sufficient ability to act as a good representative for the set of estimated transfer functions.

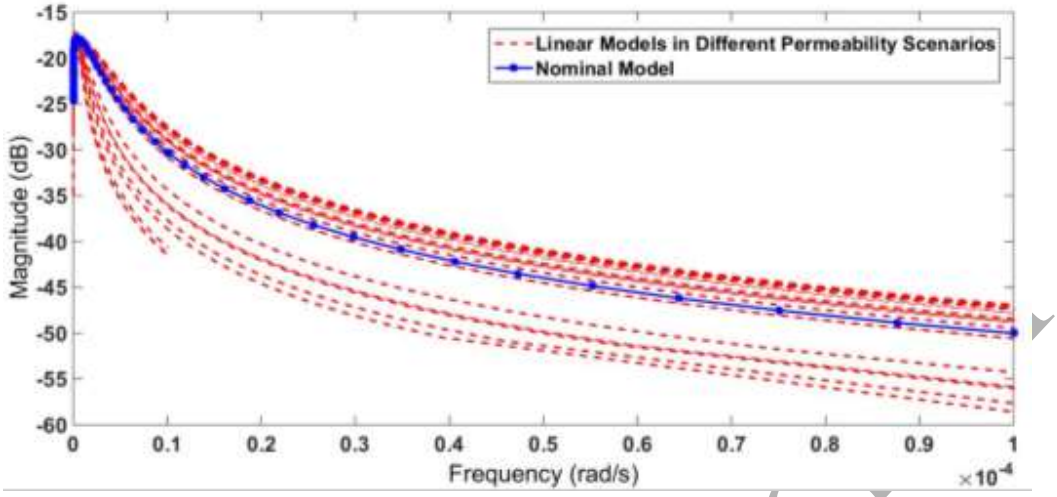

Figure 9. Bode magnitude diagrams of nominal TF and estimated TF"s, based on different permeability scenarios (Considering oil production of well #3 as the modeled output).

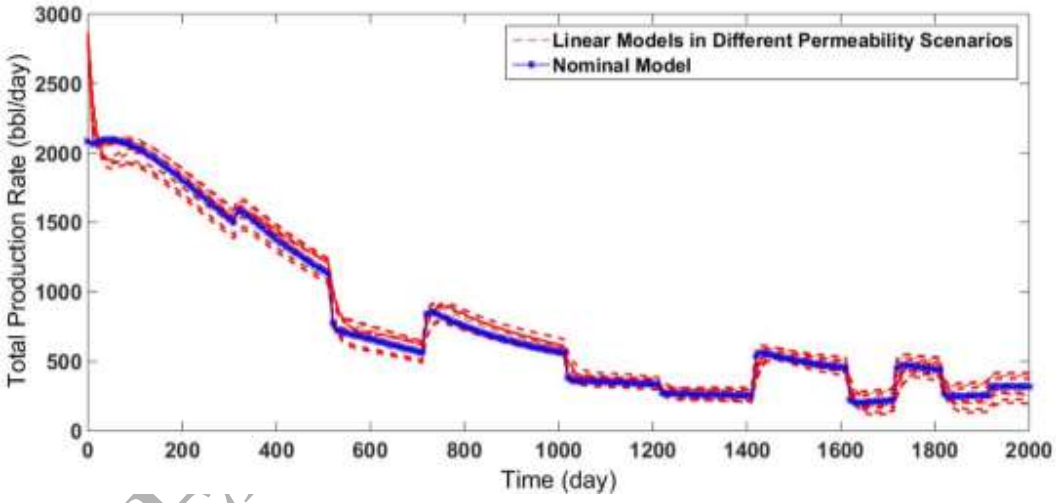

Figure 10. Time-domain response of the nominal TF and estimated TF"s, based on different permeability scenarios (Considering oil production of well #3 as the modeled output).

After generating a suitable nominal transfer function, it is time to compute an appropriate weighting transfer function, $W(s)$, by applying the described technique in section 4.3.2. Figure 11, demonstrates the differences between the nominal model and the TF"s relevant to each experiment in frequency domain in the format of Bode magnitude diagram. By observing the

presented results in Figures 12, 13 and 14, it can be perceived the 3rd-order $W(s)$ (available in Table 1) is a better option to provide an acceptable envelope over the difference curves of Figure 11, in comparison with the lower orders. As it can be seen in Figure 12, the proposed 1st-order $W(s)$ is not a suitable envelope, since it has several points of intersection with the difference curves. In addition, by comparing 2nd-order and 3rd-order options for $W(s)$, it can be found out that the existing gap between the proposed envelope and the difference curves for 3rd-order $W(s)$ is less than 2nd-order alternative. So, selecting 3rd-order $W(s)$ leads to a less conservative uncertainty model. Further analysis demonstrates that higher orders of weighting transfer functions (4th-order, 5th order and etc.) have no significant privilege over the chosen 3rd-order $W(s)$.

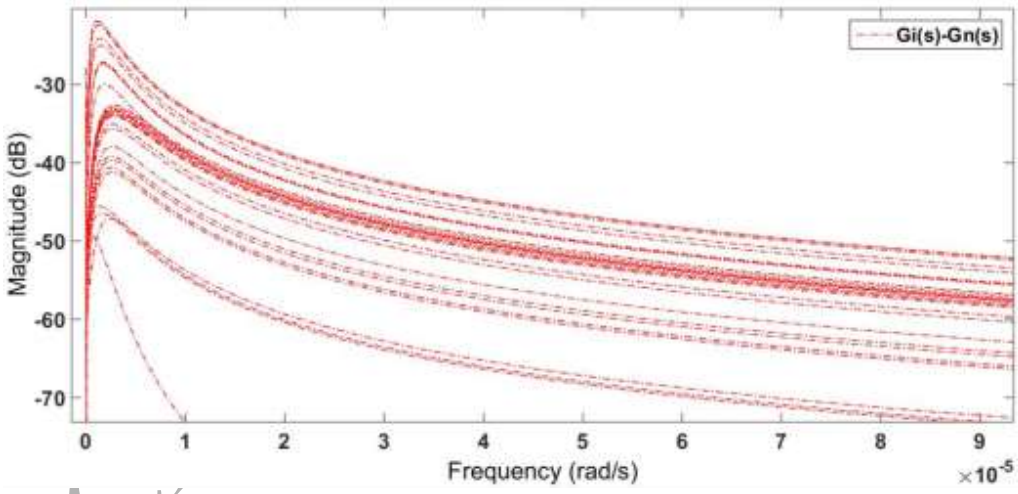

Figure 11. Bode magnitude plot of the differences between the nominal TF and estimated TF"s related to different experiments (Considering oil production of well #3 as the modeled output).

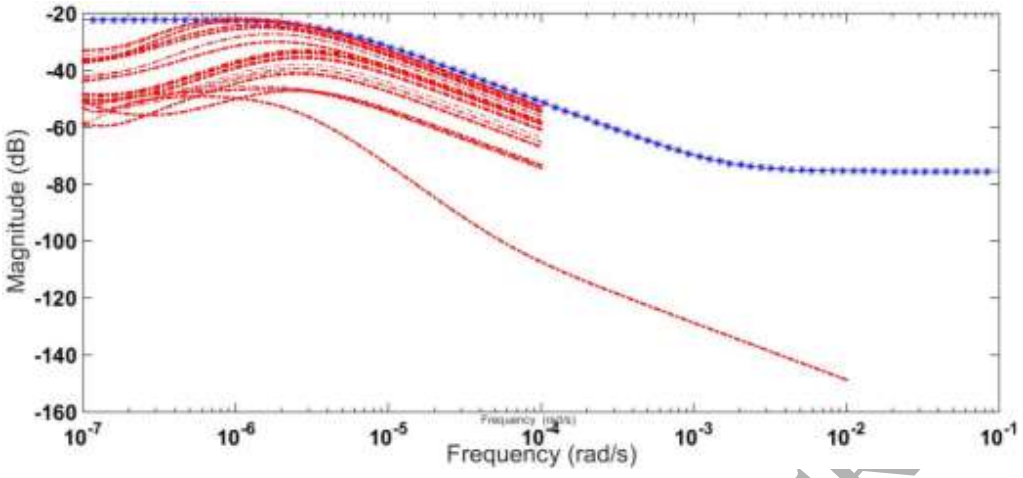

Figure 12. 1st order $W(s)$ estimation (Considering oil production of well #3 as the modeled output). Blue curve is the 1st order envelope over the models" errors (red curves).

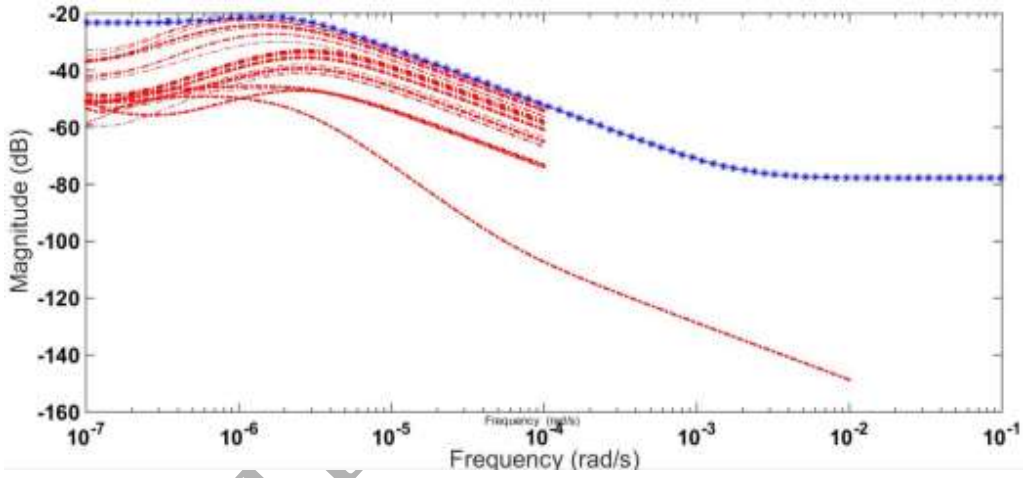

Figure 13. 2nd order $W(s)$ estimation (Considering oil production of well #3 as the modeled output). Blue curve is the 2nd order envelope over the models" errors (red curves).

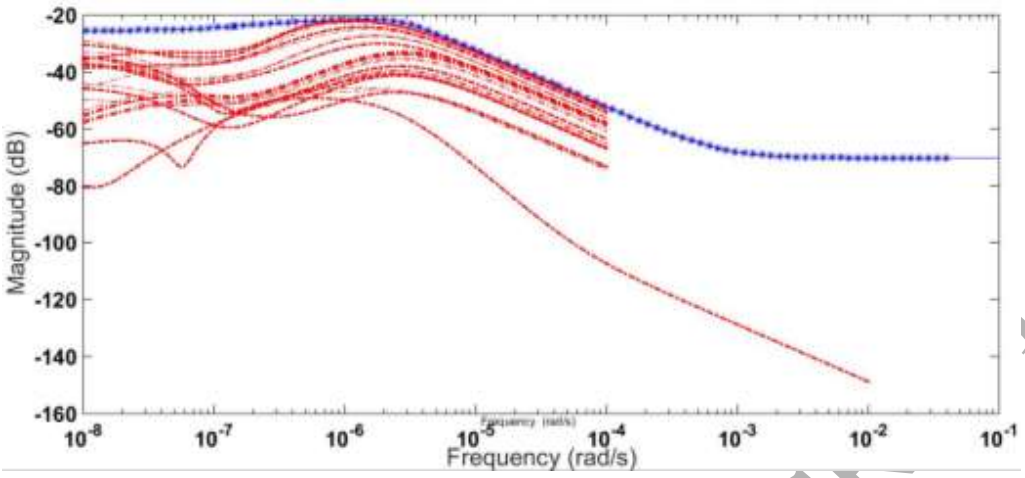

Figure 14. 3rd order $W(s)$ estimation (Considering oil production of well #3 as the modeled output). Blue curve is the 3rd order envelope over the models' errors (red curves).

To evaluate the capability of the developed modelling algorithm in reflecting the dynamic of waterflooding process in the presence of considered uncertainty, both frequency domain and time domain tests have been performed, while using random values for Δ which satisfy the condition: $\|\Delta\| \le 1$.

By setting $\Delta = +1$, which can be interpreted as the worst case for the considered uncertainty, it is obvious in Figure 15 that the summation of Bode magnitude diagram of the nominal transfer function and $W(s)$, constructs an envelope over all probable and uncertain cases ($\|\Delta\| < 1$), including the simulated experiments. This fact, is also supported by time-domain evaluation of the results as demonstrated in Figure 16. The constructed model with $G_n - \Delta$ structure is able to introduce a comprehensive set which its members are plausible dynamic representatives of oil production rate from well#3, while the values of permeability map are not precisely known. It can be seen in Figure 16 that in the presence of defined uncertainty, the probable temporal behaviors of the considered output are in a band which has been specified by upper and lower

bounds of the proposed model for waterflooding process. This information is very useful for the field experts in practical applications. Because, they can get a general view about the dynamics of the designed waterflooding process and adjust their financial expectations from the reservoir, while the available data has certain degree of uncertainty.

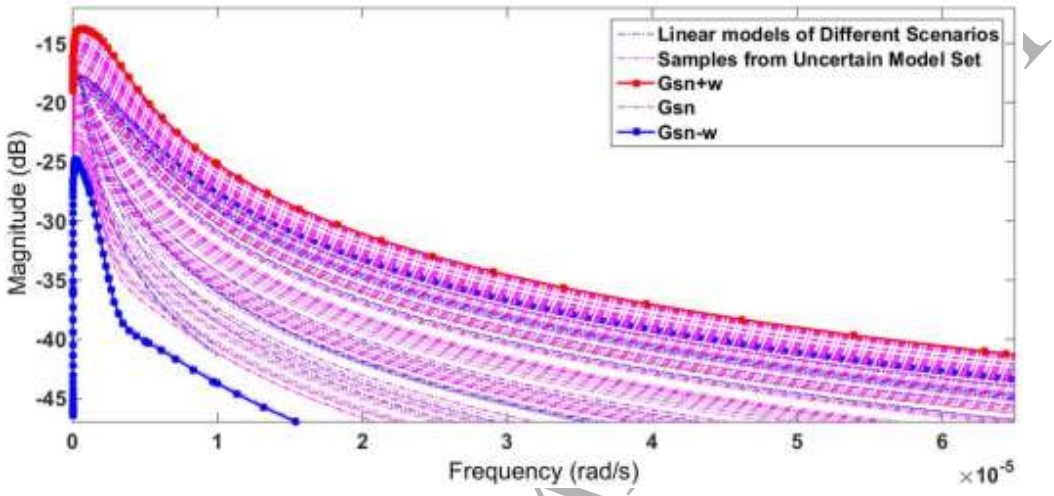

Figure 15. Samples of frequency-domain plausible scenarios (Considering oil production of well #3 as the modeled output).

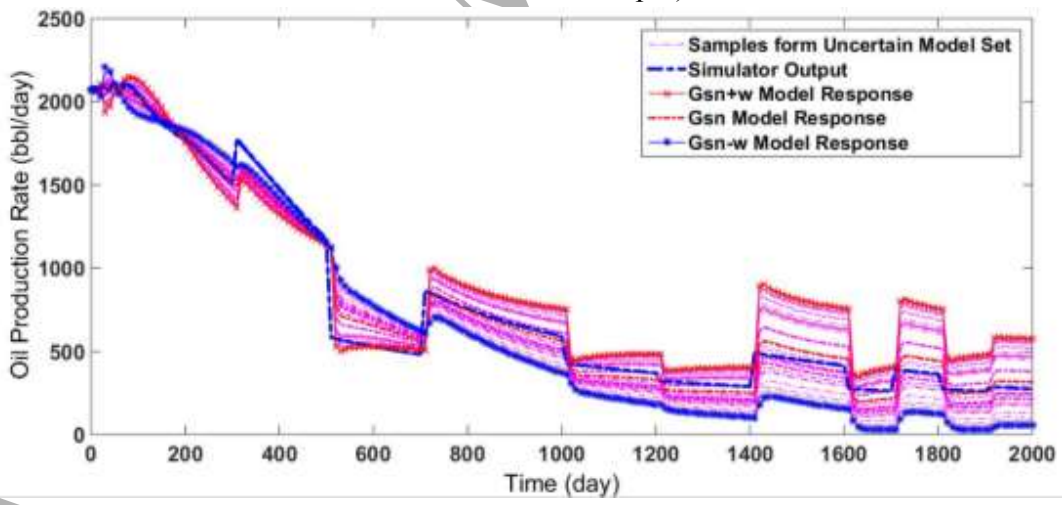

Figure 16. Samples of time-domain plausible scenarios (Considering oil production of well #3 as the modeled output).

6. Conclusion

The estimated recovery factor of hydrocarbon reservoirs can be drastically affected by unconsidered geological uncertainties. For design and implementation of efficient enhanced recovery techniques, development of valid and reliable models, which are capable to take into account the inherent reservoir uncertainty, is inevitable. These models facilitate study and evaluation of the reservoir behavior under different operational strategies. In addition, they can be used to make optimal decisions in the presence of different types of uncertainty.

In this paper, a novel methodology for modeling and quantifying the geological uncertainty impacts on waterflooding process has been developed. While a common challenging and time-consuming approach for uncertainty analysis in the reservoirs is to generate a set of different realizations, the introduced algorithm proposes a well-defined lumped configuration. The constructed model consists of nominal and uncertain parts in the form of transfer functions in frequency domain. From the system theory point of view, the nominal block is the best linear estimation of waterflooding process. Moreover, the uncertain block is a conservative approximation of the uncertainty impacts on the process.

In data gathering phase, Monte-Carlo-based experiments are designed in random values of uncertain parameters for sufficient data collection, to properly reflect the effects of uncertainty on the desired outputs. For each set of gathered input/output data, the most appropriate linear mapping in the form of transfer function is calculated. The nominal and uncertain parts of the model are obtained by using *K-means* clustering technique and also frequency analysis of Bode magnitude plot.

The observed results on 10th SPE-model#2 benchmark case study, have demonstrated that the presented algorithm has the ability to successfully model the waterflooding process dynamic, while the knowledge on the values of permeability is not exact. Analyzing time-domain

responses of the developed model for various Δ"s, introduces upper and lower bounds of the desired outputs in the presence of induced uncertainty. This information is valuable for the field experts in practice; since they will be able to make optimal and efficient decisions about the future production plans.

Another advantage of the presented modeling approach is to provide suitable models, applicable in robust control and optimization of the reservoirs. In other words, availability of such a comprehensive and lumped model provides the facilities to apply well-proven robust control theories, for appropriately adjustment of the desired reservoir output(s) while satisfying the optimization objectives in the presence of geological uncertainties. In addition, in prevalent robust optimization techniques applicable in oil reservoirs, the optimization problem is needed to be solved for all available realizations. However, the output of the presented modeling methodology- which is a lumped completely informative model- may be effectively used just for once by suitable optimization algorithms. Consequently, the optimal solutions can be achieved with much less computational load, compared to conventional robust optimization approaches.

So, we can summarize that in this paper a lumped but reliable model has been introduced based on data driven proxy reservoir modeling technique, to appropriately estimate the uncertainty impacts on production regime in hydrocarbon reservoirs during the waterflooding process. This approach helps the decision-makers to design the most effective production plans with less computational expenses and in a shorter time compared to ordinary uncertainty modeling approaches. In addition, the proposed structure is the main pre-requisite for applying any advanced and efficient robust control approach over the waterflooding process.

Acknowledgements:

The first author appreciates the assistance of Dr. Ladan Khoshnevisan for her useful technical comments, as well as her collaboration in finalizing this manuscript.

References:

1. Ahmadloo, F., Asghari, K, Gay Renouf, G., Performance prediction of waterflooding in Western Canadian heavy oil reservoirs using artificial neural network, Energy & Fuels, 24: 2520–2526, 2010.
2. Aifa, T., Neural network applications to reservoirs: Physics-based models and data models, Journal of Petroleum Science and Engineering, 123: pp.1-6, 2014.
3. Aziz, K., Settari, A.N., Petroleum reservoir simulation. London, Applied Science Publishers, 1979.
4. Caers J., On internal consistency, conditioning and models of uncertainty, 9th International Geostatistics Congress, Oslo, Norway, p. 11–5, 2012.
5. Christie, M. A., Blunt, M.J., Tenth SPE Comparative Solution Project: A Comparison of upscaling techniques, SPE 66599, SPE Reservoir Simulation Symposium, Houston, 2001.
6. de Vries, D.K., van den Hof, P.M.J., Quantification of uncertainty in transfer function estimation: a mixed probabilistic-worst-case approach, Automatica, 31(4): 543-557, 1995.
7. Douma, S.G., van den Hof, P.M.J., Relations between uncertainty structures in identification for robust control, Automatica, 41(3): 439-457, 2005.
8. Elkamel, A., An artificial neural network for predicting and optimizing immiscible flood performance in heterogeneous reservoirs, Computers & Chemical Engineering, 22(11): 1699-1709, 1998.
9. ExxonMobil Corporation, Energy Outlook to 2030, Technical report from www.exxonmobil.com/energyoutlook, 2004.
10. Fanchi, J.R., Principles of Applied Reservoir Simulation, 2nd Edition, Gulf Professional Publishing, Burlington, 2001.
11. Feyen, L., Caers, J., Quantifying geological uncertainty for flow and transport modeling in multi-modal heterogeneous formations, Advances in Water Resources, 29: 912–929, 2006.
12. Gaasø, L., Skorstad, A., Kraakenes, T., Reservoir modeling: revising uncertainty quantification and workflows, Offshore, www.offshore-mag.com, October 2014.
13. Ginting, V., Pereira, F., Rahunanthan, A., Rapid quantification of uncertainty in permeability and porosity of oil reservoirs for enabling predictive simulation, Mathematics and Computers in Simulation 99, 139–152, 2014.
14. Giuliani, C. M., Camponogara, E., Derivative-free methods applied to daily production optimization of gas-lifted oil fields. Computers and Chemical Engineering. 75: 60–64. 2015.
15. Grossmann, I.E., Apap, R.M., Calfa, B.A., Garcia-Herreros, P., Zhang, Q., Recent advances in mathematical programming techniques for the optimization of process systems under uncertainty, Computers & Chemical Engineering, 91: 3-14, 2016.
16. Gu, D. W., Petkov, P., Konstantinov, M. M., Robust Control Design with Matlab, 2nd Edition, Springer-Verlag, London, 2013.

17. Hourfar, F., Moshiri, B., Salahshoor, K., Mehrjerdi, M.Z., Pourafshary, P., Adaptive modeling of water flooding process in oil reservoirs. Journal of petroleum Science and Engineering, 146: 702-713, 2016.
18. Hourfar, F., Moshiri, B., Salahshoor, K., Elkamel, A., Real-time Management of the Waterflooding Process Using Proxy Reservoir Modeling and Data Fusion Theory. Computers & Chemical Engineering, 106: 339-354, 2017.
19. Hovadik, J., Larue, D., Predicting waterflood behavior by simulating earth models with no or limited dynamic data: From model ranking to simulating a billion-cell model, AAPG Memoir 96, 29-55, 2011.
20. Islam, A. W., Sepehrnoori, K., A review on SPE"s comparative solution projects (CSPs), Journal of Petroleum Science Research (JPSR), 2 (4): 167-180, 2013.
21. Jansen, J.D., Bosgra, O.H., van den Hof, P.M.J., Model-based control of multiphase flow in subsurface oil reservoirs, Journal of Process Control, 18(9):846-855, 2008.
22. Kanungo, T., Mount, D. M., Netanyahu, N. S., Piatko, C. D., Silverman, R., Wu, A. Y., An efficient k-Means clustering algorithm: Analysis and Implementation, IEEE Transactions on Pattern Analysis and Machine Intelligence, 24(7): 881-892, 2002.
23. Ko, S., Weyer, E., Campi, M., Non-asymptotic model quality assessment of transfer functions at multiple frequency points, IFAC 17th World Congress, Seoul, South Korea, 2008.
24. Larue, D. K., Hovadik, J., Why is reservoir architecture an insignificant uncertainty in many appraisal and development studies of clastic channelized reservoirs, Journal of Petroleum Geology, 31(4):337-366, 2008.
25. Larue, D. K., Yue, Y., How stratigraphy influences oil recovery: A comparative reservoir database study concentrating on deepwater reservoirs, the Leading Edge, 22: 332-339, 2003.
26. Le, D.H., Reynolds, A.C., Optimal choice of a surveillance operation using information theory, Computational Geoscience, 18: 505–518, 2014.
27. Li, K., Horne, R.N., Verification of decline curve analysis models for production prediction, SPE Western Regional Meeting, Irvine, California, 2005.
28. Lie, K. A., An introduction to reservoir simulation using MATLAB: User guide for the Matlab Reservoir Simulation Toolbox (MRST), SINTEF ICT, May 2014.
29. Mohaghegh, Sh., Abdulla, F., Production management decision analysis using AI-based proxy modeling of reservoir simulations – A look-back case study, Society of Petroleum Engineers, SPE-170664-MS, 2014.
30. Nashawi, I.S., Elkamel, A., Neural network model for the prediction of water aquifer dimensionless variables for edge-and bottom-water drive reservoirs, Energy & Fuels, 13 (1) :88–98, 1999.
31. Oliver, D.S, Chen, Y., Recent progress on reservoir history matching: a review, Computational Geosciences, 15(1): 185-221, 2011.
32. Park, H., Scheidt, C., Fenwick, D., Boucher, A., Caers, J., History matching and uncertainty quantification of facies models with multiple geological interpretations, Computational Geoscience, 17:609–621, 2013.
33. Sarma, P., Efficient closed-loop optimal control of petroleum reservoirs under uncertainty, PhD Thesis, Stanford University, Stanford, CA, 2006.

34. Satija, A., Caers, J., Direct forecasting of subsurface flow response from non-linear dynamic data by linear least-squares in canonical functional principal component space, Mathematics and Computers in Simulation, 99: 139–152, 2014.
35. Sayyafzadeh, M., Pourafshari, P., Rashidi, F., Increasing ultimate oil recovery by infill drilling and converting weak production wells to injection wells using streamline simulation, International Oil and Gas Conference and Exhibition in China, Society of Petroleum Engineers, Beijing, China, SPE-132125-MS, 2010.
36. Sayyafzadeh, M., Pourafshary, P., Haghighi, M., Rashidi, F., Application of transfer functions to model water injection in hydrocarbon reservoir, Journal of Petroleum Science and Engineering, 78: 139–148, 2011.
37. Scheidt C., Renard P., Caers J., Prediction-focused subsurface modeling: investigating the need for accuracy in flow-based inverse modeling, Mathematical Geoscience, 47:173–91. 2015.
38. Shook, G.M., Mitchell, K. M., A robust measure of heterogeneity for ranking earth models: The F PHI curve and dynamic Lorenz coefficient, SPE Annual Technical Conference and Exhibition, New Orleans, Louisiana, SPE-124625-MS, 2009.
39. Siraj, M. M., van den Hof, P.M.J., Jansen J.D., Robust optimization of water-flooding in oil reservoirs using risk management tools, 11th IFAC Symposium on Dynamics and Control of Process Systems Including Biosystems DYCOPS-CAB, Trondheim, Norway, 2016.
40. Tafti, T., Ershaghi, I., Rezapour, A., Ortega, A., Injection scheduling design for reduced order waterflood modeling, Society of Petroleum Engineers, SPE-165355-MS, 2013.
41. Tang, H., Liu, N., Static connectivity and heterogeneity (SCH) analysis and dynamic uncertainty estimation, International Petroleum Engineering Conference, Kuala Lumpur, Malaysia, 2008.
42. Tavallali, M.S., Karimi, I.A., Teo, K.M., Baxendale, D., Ayatollahi, Sh., Optimal producer well placement and production planning in an oil reservoir, Computers & Chemical Engineering, 55: 109-125, 2013.
43. Tavallali, M.S., Karimi, I.A., Integrated oil-field management: From well placement and planning to production scheduling, Industrial & Engineering Chemistry Research, 55 (4): 978-994, 2016a.
44. Tavallali, M.S., Karimi, I.A., Process systems engineering perspective on the planning and development of oil fields, AIChE Journal 62 (8): 2586-2604, 2016b.
45. van Essen, G., Zandvliet, M., van den Hof, P.M.J., Bosgra, O., Jansen, J. D., Robust waterflooding optimization of multiple geological scenarios, SPE Journal, 14 (01): 202–210, 2009.
46. van Essen G.M., van den Hof, P.M.J., Jansen J. D., A two-level strategy to realize life-cycle production optimization in an operational setting, SPE Journal, 18 (6): 1057-1066, 2012.
47. Yasari, E., Pishvaie, M. R., Khorasheh, F., Salahshoor, K., Kharrat, R. Application of multi-criterion robust optimization in waterflooding of oil reservoir, Journal of Petroleum Science and Engineering, 109:1–11, 2013.

48. Zhang, Y., Lu, R., Forouzanfar, F., Reynolds, A.C., Well placement and control optimization for WAG/SAG processes using ensemble-based method, Computers and Chemical Engineering, 101: 193-209, 2017.
49. Zhou H., Gómez-Hernández J.J., Li L., Inverse methods in hydrogeology: evolution and recent trends, Advances in Water Resources, 63:22–37, 2014.